ChemPubSoc Europe

DOI: 10.1002/chem.201304848

CHEMISTRY
A European Journal
Communication

Mixed-Valent Compounds

Stable Mixed-Valent Radicals from Platinum(II) Complexes of a Bis(dioxolene) Ligand

Jonathan J. Loughrey,[a, b] Stephen Sproules,[c, d] Eric J. L. McInnes,[c] Michaele J. Hardie,[a] and Malcolm A. Halcrow*[a]

Abstract: Three diplatinum(II) complexes [{PtL}$_2$(μ-thea)] (H_4thea = 2,3,6,7-tetrahydroxy-9,10-dimethyl-9,10-dihydro-9,10-ethanoanthracene) have been prepared, with diphosphine or bipyridyl "L" co-ligands. One-electron oxidation of these complexes gave radical cations containing a mixed-valent [thea$^{\cdot}$]$^{3-}$ ligand with discrete catecholate and semiquinonate centers separated by quaternary methylene spacers. The electronic character of these radicals is near the Robin–Day class II/III border determined by UV/Vis/NIR and EPR spectroscopies. Crystal-structure determinations and a DFT calculation imply that oxidation of the thea^{4-} ligand may lead to an increased through-space interaction between the dioxolene π systems.

Metal complexes of dioxolenes can exhibit a fascinating ligand-based redox chemistry, involving conversion between catecholate ("cat"), semiquinone ("sq"), and quinone ("q") ligand oxidation levels.[1–3] Complexes of dinucleating dioxolenes add another layer of complexity to this behavior with multiple metal and ligand redox sites,[2–4] which may give rise to ligand-based mixed valency.[5] One example is 4,4′-bis(catechol) (H_4bis(cat), Scheme 1), whose derivatives form delocalized radicals at the sq/cat oxidation state, but are spin coupled at the sq/sq level reflecting formal oxidation of the central C–C bond.[6–8] Conversely, cat/sq radicals generated from spiro^{4-} complexes (H_4spiro = 3,3,3′,3′-tetramethyl-1,1′-spiro-bis{5,6-dihydroxyindane}, Scheme 1) are localized on individual dioxolene rings,[2] with electron hopping between the dioxolene groups occurring near the EPR timescale.[9] Transition-metal dioxolene complexes can also exhibit valence tautomerism and spin-transition equilibrium involving metal⇌ligand charge transfer,[10] but few examples of these phenomena in bis(dioxolene) ligand systems have been reported to date.[2,9,11]

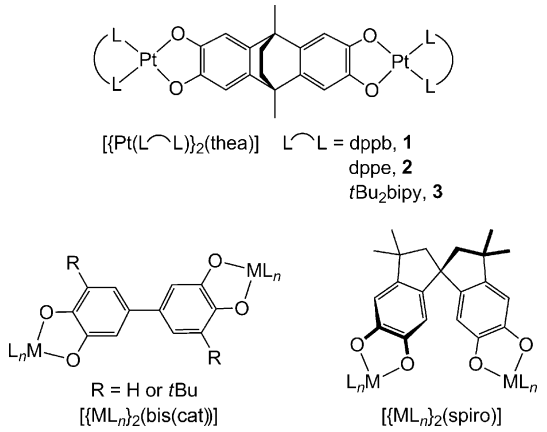

Scheme 1. Compounds reported herein and other complexes referred to in the discussion. Co-ligand abbreviations: dppb = 1,2-bis(diphenylphosphino)-benzene; dppe = 1,2-bis(diphenyl-phosphino)ethane; and tBu$_2$bipy = 4,4′-bis(*tert*-butyl)-2,2′-bipyridyl.

Herein, we report the redox chemistry of 2,3,6,7-tetrahydroxy-9,10-dimethyl-9,10-dihydro-9,10-ethanoanthracene (H_4thea) when complexed to platinum(II) (**1**–**3**, Scheme 1). Others have used thea^{4-} as a component in metallacycle and cage complexes, but the redox chemistry of those products was not reported.[12,13] The dimethyl-bicyclo[2.2.2]octyl spacer prevents formal conjugation of the thea^{n-} dioxolene groups but places them close in space. Therefore, we predicted that the cat/sq species [thea$^{\cdot}$]$^{3-}$ should exhibit mixed-valence behavior intermediate between [bis(cat)$^{\cdot}$]$^{3-}$ and [spiro$^{\cdot}$]$^{3-}$ (Scheme 1).

The synthesis of compounds **1**–**3** was achieved by reacting H_4thea with two equivalents of preformed [PtCl$_2$L] (L = dppb, dppe, or tBu$_2$bipy) in the presence of base. The complexes can be handled in air in the solid state and in solution, but must be stored under an inert atmosphere for extended periods. X-ray structure determinations of **1** and **2** were achieved from solvate crystals grown from dichloromethane/pentane (Figure 1). Although both structures are crystallographically

[a] Dr. J. J. Loughrey, Prof. M. J. Hardie, Prof. M. A. Halcrow
School of Chemistry, University of Leeds
Woodhouse Lane, Leeds, LS2 9JT (UK)
Fax: (+44) 113-343-6565
E-mail: m.a.halcrow@leeds.ac.uk

[b] Dr. J. J. Loughrey
Current address: Department of Chemistry and Biochemistry
University of Arizona, P.O. Box 210041
1306 East University Blvd., Tucson, AZ 85721-0041 (USA)

[c] Dr. S. Sproules, Prof. E. J. L. McInnes
School of Chemistry and Photon Science Institute
University of Manchester, Oxford Road, Manchester, M13 9PL (UK)

[d] Dr. S. Sproules
Current address: School of Chemistry, University of Glasgow
Joseph Black Building. University Avenue, Glasgow, G12 8QQ (UK)

Supporting information for this article is available on the WWW under http://dx.doi.org/10.1002/chem.201304848.

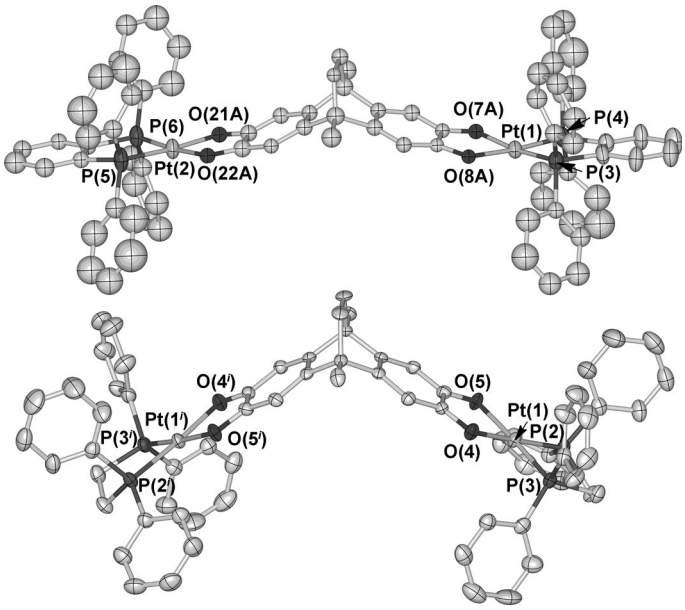

Figure 1. "A" disorder site of the [{Pt(dppb)}$_2$(thea)] molecule in [**1**·xC$_5$H$_{12}$×(4−x)CH$_2$Cl$_2$] (top),[12] and the [{Pt(dppe)}$_2$(thea)]$^+$ cation in [**2**]PF$_6$·3CH$_2$Cl$_2$ (bottom). Displacement ellipsoids are at the 50% probability level, and all hydrogen atoms have been omitted for clarity. Symmetry code: (*i*) 3/2−x, 1/2−y, z. Additional crystallographic Figures and Tables are given in the Supporting Information.[16]

non-routine,[14] the metric parameters about the thea^{4-} ligands confirm that the dioxolene rings are at the catecholate oxidation level ($-1.7(3) \geq \Delta \geq -2.1(2)$,[15] Table 1). The dihedral angle between the thea^{4-} dioxolene groups (θ, Table 1) is approximately 10° larger in **2** than in **1**, showing that there is some conformational flexibility in the thea^{4-} framework.

Cyclic and differential pulse voltammetry of **1**–**3** in CH$_2$Cl$_2$/0.5 M nBu$_4$NPF$_6$ at 298 K revealed two chemically reversible low-potential oxidations at -0.37 ± 0.02 and -0.11 ± 0.02 V versus [FeCp$_2$]/[FeCp$_2$]$^+$.[16] These were assigned to the [thea]$^{4-} \rightleftharpoons$[thea$^{\cdot}$]$^{3-} \rightleftharpoons$[thea$^{\cdot}$]$^{2-}$ (cat/cat⇌cat/sq⇌sq/sq) redox series. The separation of these processes (ΔE) is 250 ± 20 mV, between complexes of bis(cat)$^{4-}$ (ΔE = 320–500 mV)[2,6,7] and of spiro^{4-} (140–170 mV).[2,9] The subsequent [thea$^{\cdot}$]$^{2-} \rightleftharpoons$[thea$^{\cdot}$]$^{-} \rightleftharpoons$[thea]^0 (sq/sq⇌sq/q⇌q/q) oxidations occurred near + 0.75 V, were more closely separated ($\Delta E \leq 110$ mV) and were only partly reversible at room temperature.

The green oxidized products [**1**]$^+$ and [**2**]$^+$, and purple [**3**]$^+$, can be generated by treatment of the neutral precursors with one equivalent of [FeCp$_2$]PF$_6$ in CH$_2$Cl$_2$. Solutions of [**1**]$^+$ and [**2**]$^+$ are stable for hours at 298 K under an inert atmosphere, which allowed [**1**]PF$_6$ and [**2**]PF$_6$ to be isolated and crystallized (see below), but [**3**]PF$_6$ decomposes slowly under those conditions. The oxidations were monitored by UV/Vis/NIR titrations, which proceeded isosbestically for **1** and **2** (Figure 2). In both cases, ingrowth of a new intervalence charge transfer (IVCT)

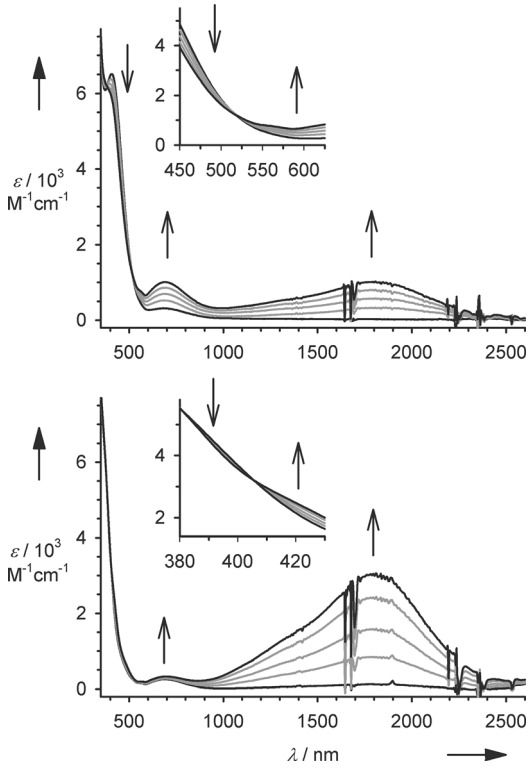

Figure 2. UV/Vis/NIR titrations for the chemical oxidation of **1** (top) and **2** (bottom) by up to one equivalent of [FeCp$_2$]PF$_6$ (CH$_2$Cl$_2$, 296 K). The spectra of pure **1**, [**1**]$^+$, **2**, and [**2**]$^+$ are highlighted as black lines, whereas the intermediate stoichiometries are in grey. Isosbestic points are shown as insets.[16]

Table 1. Selected metric parameters from the crystal structures in this work. Δ is a bond-valence sum parameter giving the oxidation state of dioxolene groups, which takes the values of 0, −1, and −2 for the q, sq, and cat levels, respectively.[15] θ is the dihedral angle between the least squares planes of the thea^{n-} dioxolene rings. More detailed information about the structures is given in the Supporting Information.

	Pt–O [Å]	Pt–P [Å]	Δ	θ [°]
1	1.98(2)–2.05(2)	2.201(3)–2.207(3)	$-1.7(3) \geq \Delta \geq -1.9(2)$[a]	140.8(5)–141.1(5)[a]
2 molecule A	2.026(8)–2.048(8)	2.202(4)–2.227(3)	−1.77(15), −2.1(2)	130.8(5)
molecule B	2.006(13)–2.049(9)	2.205(4)–2.236(4)	−1.86(14), −2.1(2)	131.1(6)
molecule C	2.034(9)–2.071(15)	2.195(6)–2.222(4)	−1.90(15)[b]	129.8(9)–131.5(6)[a]
[**2**]PF$_6$[c]	2.042(4), 2.060(4)	2.2101(14), 2.2197(14)	−1.57(15)	117.14(11)

[a] Range of values given for disorder sites in this residue.[14] [b] Δ for the second Pt/dioxolene center in this molecule was not determined because of restraints applied in the crystallographic refinement. [c] There is only one unique Pt/dioxolene center in this crystal structure.[14]

transition at λ_{max} = 1810 nm with at least one low-wavelength shoulder was observed, along with a smaller increase in intensity of the dioxolene→L (L = dppb or dppe) ligand-to-ligand charge transfer (LLCT) band near 690 nm.[7] The intensity of the IVCT band is around three times greater in [**2**]$^+$ than in [**1**]$^+$. An IVCT band with λ_{max} = 1917 nm is also formed during the oxidation of **3**, reaching

$\varepsilon_{max} = 6.3 \times 10^3\ M^{-1}\,cm^{-1}$ for $[\mathbf{3}]^+$, which is twice as intense as that exhibited by $[\mathbf{2}]^+$ (Figure 2). That titration was not isosbestic, however, which indicates slow decomposition of $[\mathbf{3}]^+$ under these conditions.

The width at half height, $\Delta\nu_{1/2}$, of the IVCT bands in $[\mathbf{1}]^+$ and $[\mathbf{2}]^+$ is $\leq 2300\ cm^{-1}$, taking account of the low-wavelength shoulder. That is smaller than predicted by Equation (1) for $[\mathbf{1}]^+$ and $[\mathbf{2}]^+$, which gives $\Delta\nu_{1/2} \approx 3550\ cm^{-1}$ for a class II mixed-valent system with an IVCT maximum of 1810 nm ($E = 5525\ cm^{-1}$).[17]

$$\Delta\nu_{1/2} = (2310E)^{1/2} \quad (1)$$

Although this criterion should be applied with care, the $[thea^{\cdot}]^{3-}$ framework is clearly approaching the class III formalism. In the class III limit, the electron-coupling energy H_{AB} for $[\mathbf{1}]^+$ and $[\mathbf{2}]^+$ is approximately $1150\ cm^{-1}$ according to Equation (2):[5,17]

$$H_{AB} = {}^1/_2\Delta\nu_{1/2} \quad (2)$$

That is comparable to cyclophane radical ions and related species, which show through-space coupling between stacked aromatic rings.[18] Solutions of $[\mathbf{2}]^+$ exhibit a correlation between the IVCT maximum and the donor number of the solvent,[19] in the order DMF ($\lambda_{max} = 1883$ nm) > THF (1847) > acetone (1829) > CH_2Cl_2 (1810). The maximum variation in IVCT energy between these solvents ($215\ cm^{-1}$) is smaller than expected for a class II organic radical,[20] and again implies a degree of delocalization between the $[thea^{\cdot}]^{3-}$ dioxolene groups.[5] The IVCT linewidth $\Delta\nu_{1/2}$ does not vary significantly in these spectra, but the relative intensities of the IVCT band and the LLCT absorption near 700 nm show a much stronger solvent dependence.[16]

The S band and X band EPR spectra of $[\mathbf{1}]^+$ and $[\mathbf{2}]^+$ in CH_2Cl_2/THF 10:1 fluid solution are very similar, with g values close to that of the free electron (Table 2 and Figure 3). Although hyperfine coupling was not clearly resolved, features on the S-band line shape could be modelled by considering hyperfine coupling to two ^{195}Pt ($I = {}^1/_2$, 34% abundant) and four ^{31}P ($I = {}^1/_2$, 100% abundant) nuclei. The spectrum of $[\mathbf{3}]^+$ contains five resolved lines that more obviously arise from hyperfine coupling to two ^{195}Pt nuclei. This demonstrates electron hopping between the $[thea^{\cdot}]^{3-}$ dioxolene rings that is rapid on the EPR timescale at these temperatures. The X-band line widths of $[\mathbf{1}]^+$ and $[\mathbf{2}]^+$ are almost invariant between 200–300 K, but the spectrum of $[\mathbf{3}]^+$ broadens considerably below 230 K, which could indicate the slowing of this electron hopping[9] and/or aggregation of the complex in solution (see below).[16] In contrast, frozen solution X-band spectra of $[\mathbf{1}]^+$–$[\mathbf{3}]^+$ are near-axial and show coupling to just one ^{195}Pt nucleus, and for $[\mathbf{1}]^+$ and $[\mathbf{2}]^+$, two ^{31}P nuclei (Figure 3). Therefore, electron hopping between their dioxolene groups is frozen out, apparently coinciding with freezing of the solvent medium.[9] Although the hyperfine coupling for $[\mathbf{3}]^+$ is poorly resolved in the frozen solution spectrum, the g anisotropy and ^{195}Pt couplings in $[\mathbf{3}]^+$ are over double those in $[\mathbf{1}]^+$ and $[\mathbf{2}]^+$. This indicates a greater Pt contribution to the frontier orbital in the presence of the more strongly π-accepting tBu$_2$bipy ligand.[21]

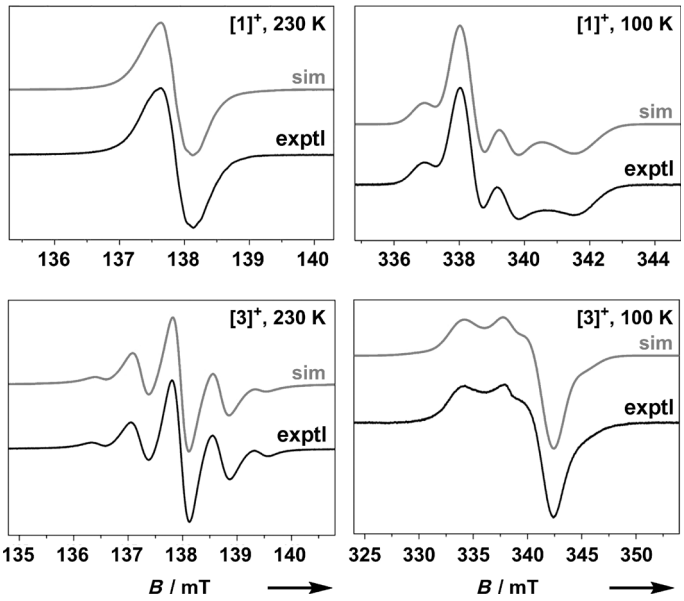

Figure 3. Fluid solution S band and frozen solution X band EPR spectra of $[\mathbf{1}]^+$ and $[\mathbf{3}]^+$ in CH_2Cl_2/THF 10:1. Simulation parameters are given in Table 2.[16]

Table 2. Simulated EPR spectroscopic parameters for $[\mathbf{1}]^+$–$[\mathbf{3}]^+$ in CH_2Cl_2/THF 10:1 solution. Hyperfine couplings are related to ^{195}Pt, and are reported in $10^{-4}\ cm^{-1}$.

	210 K g ($A^{[a]}$)	100 K g_1 ($A_1^{[b]}$)	g_2 ($A_2^{[b]}$)	g_3 ($A_3^{[b]}$)
$[\mathbf{1}]^{+[c]}$	2.0011 (4.9)	2.0045 (20)	2.0031 (19)	1.9844 (−10)
$[\mathbf{2}]^{+[c]}$	2.0012 (4.7)	2.0055 (19.5)	2.0032 (19)	1.9833 (−10)
$[\mathbf{3}]^+$	2.0019 (13.5)	2.0292 (48)	1.9872 (48)	1.9796 (40)

[a] Coupling to two ^{195}Pt nuclei. [b] Coupling to one ^{195}Pt nucleus. [c] Additional superhyperfine coupling of $1–3 \times 10^{-4}\ cm^{-1}$ to ^{31}P nuclei can also be extracted from the line shapes of these spectra.

Single-crystal X-ray structures were obtained of $[\mathbf{2}]PF_6 \cdot 3\,CH_2Cl_2$ and a solvate of $[\mathbf{1}]PF_6$, although the latter structure was of too low resolution for a detailed analysis of its metric parameters.[14] The complex cation in $[\mathbf{2}]PF_6 \cdot 3\,CH_2Cl_2$ has crystallographic C_2 symmetry, meaning that the oxidized and unoxidized dioxolene groups are crystallographically equivalent (Figure 1). Although the bond lengths to the Pt atom are indistinguishable from the neutral complexes, the metric parameters in the unique dioxolene center are consistent with a singly oxidized $[thea^{\cdot}]^{3-}$ ligand ($\Delta = -1.57(15)$, Table 1; the expected value is -1.5[15]). The dihedral angle between the dioxolene groups (θ) in $[\mathbf{2}]^+$ is contracted to 117.14(11)°, which is approximately 14° lower than in **2** (Table 1; the corresponding values for the two unique complex cations in $[\mathbf{1}]PF_6$ are 108.7(5) and 112.8(7)°). Although they are not isomorphous, in both structures the radical cations associate into nested dimers

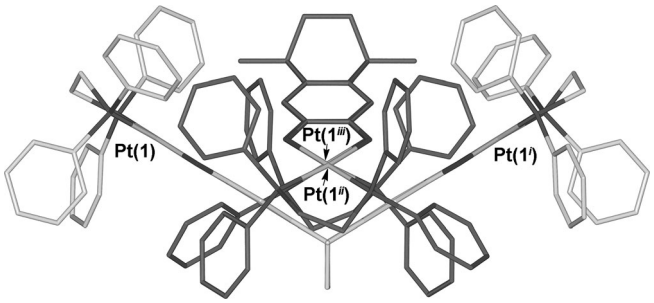

Figure 4. View of the association of the radical cations in [**2**]PF_6·3CH_2Cl_2 into nested dimers, generated from the unique half-molecule by crystallographic S_4 symmetry. The carbon atoms of the two molecules have grey and black colors, and hydrogen atoms have been omitted for clarity. Pt(1^{ii}) is at the front of the figure, whereas Pt(1^{iii}) is directly behind it. Symmetry codes: (*i*) 3/2−*x*, 1/2−*y*, *z*; (*ii*) 1/2+*y*, 1−*x*, 1−*z*; (*iii*) 1−*y*, −1/2+*x*, 1−*z*.

(Figure 4). The assignment of these dimers as charge-transfer assemblies is uncertain, because there are no interatomic contacts between the nested molecules shorter than the sum of their van der Waals radii. However, a dimerization equilibrium of this type could explain the EPR line broadening observed for [**3**]$^+$ below 230 K.[16] Notably, unoxidized **1** and **2** do not dimerize in this manner in the crystals of those compounds. The PF_6^- ions in both radical structures only associate with the cations through peripheral van der Waals contacts.[14,16]

A DFT calculation of the model complex [{Pt(bipy)}$_2$(thea)] showed that the HOMO lies predominantly on the thea^{4-} ligand and has π-antibonding character between the two dioxolene rings.[16] The reduced θ values in [**1**]PF_6 and [**2**]PF_6 compared to **1** and **2** (Table 1) are consistent with depopulation of this HOMO upon oxidation, which would strengthen any bonding interaction between the dioxolene groups. The HOMO−1 is the corresponding in-phase combination between the thea^{4-} dioxolene rings. The calculated energy gap between the HOMO and HOMO−1, 0.24 V, is a good match for the electrochemical separation between the cat/sq oxidations in **1**–**3** ($\Delta E \approx 250$ mV).

In conclusion, oxidation of **1**–**3** gave [thea$^{\cdot}$]$^{3-}$ radical derivatives. Although their dioxolene centers are not directly conjugated, [**1**]$^+$–[**3**]$^+$ show electron hopping between the dioxolene rings in fluid solution by EPR, and a degree of electron delocalization that is comparable to cyclophane-derived radicals.[18] The strength of this electron coupling may reflect the proximity of the dioxolene rings, which are only 2.4 Å apart at their closest approach in [**2**]PF_6. More detailed spectroscopic and theoretical studies are in progress to characterize the other redox states of **1**–**3** and to clarify the electronic structures of radical species based on thea^{n-} and related bis- and tris(dioxolenes).

Experimental Section

Synthetic procedures and characterization data for **1**–**3**, as well as details of the instrumentation and computational procedures used for the spectroscopic and electrochemical measurements, crystal-structure determinations, and DFT calculations, are given in the Supporting Information.[16]

Acknowledgements

This work was supported by the EPSRC. We thank Diamond Light Source for access to beamline I19 (MT8517) that contributed to the results presented herein.

Keywords: charge transfer · dioxolenes · mixed-valent compounds · platinum · radical ions

[1] C. G. Pierpoint, C. W. Lange, *Prog. Inorg. Chem.* **1993**, *41*, 331–442.
[2] A. Dei, D. Gatteschi, C. Sangregorio, L. Sorace, *Acc. Chem. Res.* **2004**, *37*, 827–835.
[3] J. S. Miller, K. S. Min, *Angew. Chem.* **2009**, *121*, 268–278; *Angew. Chem. Int. Ed.* **2009**, *48*, 262–272.
[4] Other bis(dioxolene) radical complexes have also been investigated as molecular magnets: a) A. Caneschi, A. Dei, H. Lee, D. A. Shultz, L. Sorace, *Inorg. Chem.* **2001**, *40*, 408–411; b) D. A. Shultz, S. H. Bodnar, H. Lee, J. W. Kampf, C. D. Incarvito, A. L. Rheingold, *J. Am. Chem. Soc.* **2002**, *124*, 10054–10061; c) D. A. Shultz, R. M. Fico jr. , S. H. Bodnar, R. K. Kumar, K. E. Vostrikova, J. W. Kampf, P. D. Boyle, *J. Am. Chem. Soc.* **2003**, *125*, 11761–11771; d) J. C. Sloop, D. A. Shultz, T. Coote, B. Shepler, U. Sullivan, J. W. Kampf, P. D. Boyle, *J. Phys. Org. Chem.* **2012**, *25*, 314–321.
[5] a) J. Hankache, O. S. Wenger, *Chem. Rev.* **2011**, *111*, 5138–5178; b) A. Heckmann, C. Lambert, *Angew. Chem.* **2012**, *124*, 334–404; *Angew Chem. Int. Ed.* **2012**, *51*, 326–392.
[6] a) L. F. Joulié, E. Schatz, M. D. Ward, F. Weber, L. J. Yellowlees, *J. Chem. Soc. Dalton Trans.* **1994**, 799–804; b) A. M. Barthram, Z. R. Reeves, J. C. Jeffery, M. D. Ward, *J. Chem. Soc. Dalton Trans.* **2000**, 3162–3169.
[7] J. Best, I. V. Sazanovich, H. Adams, R. D. Bennett, E. S. Davies, A. J. H. M. Meijer, M. Towrie, S. A. Tikhomirov, O. V. Bouganov, M. D. Ward, J. A. Weinstein, *Inorg. Chem.* **2010**, *49*, 10041–10056.
[8] A. Bencini, C. A. Daul, A. Dei, F. Mariotti, H. Lee, D. A. Shultz, L. Sorace, *Inorg. Chem.* **2001**, *40*, 1582–1590.
[9] K. G. Alley, G. Poneti, P. S. D. Robinson, A. Nafady, B. Moubaraki, J. B. Aitken, S. C. Drew, C. Ritchie, B. F. Abrahams, R. K. Hocking, K. S. Murray, A. M. Bond, H. H. Harris, L. Sorace, C. Boskovic, *J. Am. Chem. Soc.* **2013**, *135*, 8304–8323.
[10] a) C. G. Pierpont, *Coord. Chem. Rev.* **2001**, *216–217*, 99–125; b) D. N. Hendrickson, C. G. Pierpont, *Top. Curr. Chem.* **2004**, *234*, 63–95; c) C. G. Pierpont, *Inorg. Chem.* **2011**, *50*, 9766–9772.
[11] a) A. Beni, A. Dei, D. A. Shultz, L. Sorace, *Chem. Phys. Lett.* **2006**, *428*, 400–404; b) M. Affronte, A. Beni, A. Dei, L. Sorace, *Dalton Trans.* **2007**, 5253–5259; c) K. G. Alley, G. Poneti, J. B. Aitken, R. K. Hocking, B. Moubaraki, K. S. Murray, B. F. Abrahams, H. H. Harris, L. Sorace, C. Boskovic, *Inorg. Chem.* **2012**, *51*, 3944–3946.
[12] P. Thuéry, B. Masci, *Supramol. Chem.* **2003**, *15*, 95–99.
[13] B. F. Abrahams, N. J. FitzGerald, R. Robson, *Inorg. Chem.* **2010**, *49*, 5953–5956.
[14] The complex molecule in **1**·*x*C_5H_{12}·(4−*x*)CH_2Cl_2 is disordered across a noncrystallographic mirror plane. The crystal also contains channels of disordered solvent. The asymmetric unit of **2**·0.67H_2O·2.07CH_2Cl_2 contains three unique complex molecules, which also contain some disorder. Solvated [**1**]PF_6 contains two unique complex half-molecules with crystallographic C_2 symmetry. The PF_6^- ions occupy defined lattice sites, but the unit cell contains 26% disordered void space making the crystals poor diffractors of X-rays. The complex cation in [**2**]PF_6·3CH_2Cl_2 also has crystallographic C_2 symmetry. The anions and solvent lie in disordered sheets between layers of the cations, although the anion sites were clearly resolved in the Fourier map.[16]
[15] O. Carugo, C. B. Castellani, K. Djinović, M. Rizzi, *J. Chem. Soc. Dalton Trans.* **1992**, 837–841.
[16] Additional Tables and Figure of the voltammetry, EPR, and UV/Vis/NIR data, the crystal structures, and the DFT calculation are given in the Supporting Information.

[17] K. D. Demadis, C. M. Hartshorn, T. J. Meyer, *Chem. Rev.* **2001**, *101*, 2655 – 2685.
[18] See, for example: a) D. Sun, S. V. Rosokha, J. K. Kochi, *J. Am. Chem. Soc.* **2004**, *126*, 1388 – 1401; b) P. H. Dinolfo, V. Coropceanu, J. L. Brédas, J. T. Hupp, *J. Am. Chem. Soc.* **2006**, *128*, 12592 – 12593.
[19] Y. Marcus, *Chem. Soc. Rev.* **1993**, *22*, 409 – 416.
[20] See, for example: S. F. Nelsen, D. A. Trieber II, R. F. Ismagilov, Y. Teki, *J. Am. Chem. Soc.* **2001**, *123*, 5684 – 5694.
[21] a) E. J. L. McInnes, R. D. Farley, S. A. Macgregor, K. J. Taylor, L. J. Yellowlees, C. C. Rowlands, *J. Chem. Soc. Faraday Trans.* **1998**, *94*, 2985 – 2991; b) E. J. L. McInnes, R. D. Farley, C. C. Rowlands, A. J. Welch, L. Rovatti, L. J. Yellowlees, *J. Chem. Soc. Dalton Trans.* **1999**, 4203 – 4208.

Received: December 11, 2013
Published online on February 2, 2014

